J. Physiol. (1984), **349**, *pp.* 227–247
With 12 *text-figures*
Printed in Great Britain

IONIC BASIS FOR THE ELECTRORESPONSIVENESS AND OSCILLATORY PROPERTIES OF GUINEA-PIG THALAMIC NEURONES *IN VITRO*

BY HENRIK JAHNSEN* AND RODOLFO LLINÁS

From the Department of Physiology & Biophysics, New York University Medical Center, 550 First Avenue, New York, NY 10016 U.S.A.

(*Received 1 June 1983*)

SUMMARY

1. The ionic requirements for electroresponsiveness in thalamic neurones were studied using *in vitro* slice preparations of the guinea-pig diencephalon.

2. Analysis of the current–voltage relationship in these neurones revealed delayed and anomalous rectification.

3. Substitution of Na^+ with choline in the bath or addition of tetrodotoxin (TTX) abolished the fast spikes and the plateau potentials, described in the accompanying paper.

4. Ca^{2+} conductance blockage with Co^{2+}, Cd^{2+} or Mn^{2+}, or replacement of Ca^{2+} by Mg^{2+} abolished the low-threshold spikes (l.t.s.). Substitution with Ba^{2+} did not significantly increase the duration of the l.t.s., suggesting that under normal conditions the falling phase of this response is brought about by inactivation of the Ca^{2+} conductance.

5. The after-hyperpolarization (a.h.p.) following fast spikes was markedly reduced in amplitude and duration by bath application of Cd^{2+}, Co^{2+} or Mn^{2+}, indicating that a large component of this response is generated by a Ca^{2+}-dependent K^+ conductance ($g_{K[Ca]}$).

6. Following hyperpolarizing current pulses, the membrane potential showed a delayed return to base line. This delay is produced by a transient K^+ conductance as it can be modified by changing the drive force for K^+.

7. Presumptive intradendritic recording demonstrated high-threshold Ca^{2+} spikes (h.t.s.s) which activate a $g_{K[Ca]}$. Such h.t.s.s were also seen at the somatic level when K^+ conductance was blocked with 4-aminopyridine.

8. It is proposed that the intrinsic biophysical properties of thalamic neurones allow them to serve as relay systems and as single cell oscillators at two distinct frequencies, 9–10 and 5–6 Hz. These frequencies coincide with the α and θ rhythms of the e.e.g. and, in the latter case, with the frequency of Parkinson's tremor.

* Present address: Institute of Neurophysiology, Blegdamsvej 3C, DK-2200 Copenhagen N, Denmark.

INTRODUCTION

The electrophysiological characteristics of *in vitro* mammalian thalamic neurones were reported in the previous paper (Jahnsen & Llinas, 1984). Here we describe the extracellular ionic requirements and some of the pharmacological properties of their electroresponsiveness. It will be shown that in addition to the membrane conductances underlying the generation of the fast action potentials, thalamic neurones have other voltage-dependent ionic conductances, in particular a marked early K^+ conductance (I_A), a low- and a high-threshold Ca^{2+} conductance, a non-inactivating Na^+ conductance, and a Ca^{2+}-dependent K^+ conductance ($g_{K[Ca]}$). These conductances represent the basis for two firing properties found in thalamic neurones, the burst and the tonic firing condition. The oscillatory attributes which characterize these cells may be considered a third functional state not necessarily related to their integrative activity, but rather an expression of an inherent pace-maker property. Part of these findings have been published as preliminary reports (Llinás & Jahnsen, 1982; Jahnsen & Llinás, 1982).

METHODS

The methods are similar to those described in the accompanying paper (Jahnsen & Llinás, 1984) and in previous publications (Llinás & Sugimori, 1980*a*, *b*). Drug and ionic substitutes were utilized as follows.

Control solution (in mM): NaCl, 130; KCl, 5; $MgSO_4$, 1·3; $CaCl_2$, 2·4; KH_2PO_4, 1·2; $NaHCO_3$, 19 and glucose, 10. In the Na^+-free solution, NaCl was substituted with choline Cl on an equimolar basis. In experiments where Cd^{2+}, Co^{2+}, Mn^{2+} or Ba^{2+} was used, KH_2PO_4 was replaced with KCl and in the case of Ba^{2+}, $MgCl_2$ was used instead of $MgSO_4$. In these experiments Ca^{2+} was usually either reduced or omitted in order to keep the total concentration of divalent cations constant. When the concentration of K^+ was raised or lowered, the concentration of Na^+ was changed accordingly to maintain the osmolarity of the solution. TTX was used in a concentration of 1 μg/ml and 4-aminopyridine at 0·5 mM.

RESULTS

Electrical properties of thalamic neurones

Study of the passive electrical properties of thalamic neurones was approached using square-wave and double-ramp current injection. The square current pulse technique revealed non-linear membrane properties, even for voltage variations as small as 10 mV. The potentials generated by hyperpolarizing and depolarizing current steps for a cell held near −53 mV (resting potential −70 mV) are shown in Fig. 1*A*. For a small outward current, a depolarizing potential with a smooth charging trajectory was usually observed. Larger current injections (e.g. 0·5 nA) generated an early break in the depolarizing trajectory followed by a flat or slightly rising membrane potential change culminating in the generation of an action potential.

Following inward current pulses, a reduction of the membrane resistance was often noted and a rebound response was generally observed at the break of the hyperpolarizing pulse. The current–voltage relation obtained by injections of successively larger de- and hyperpolarizing square current pulses (such as shown in *A*) are plotted for four cells in Fig. 1*B*. In these examples, as well as in other neurones

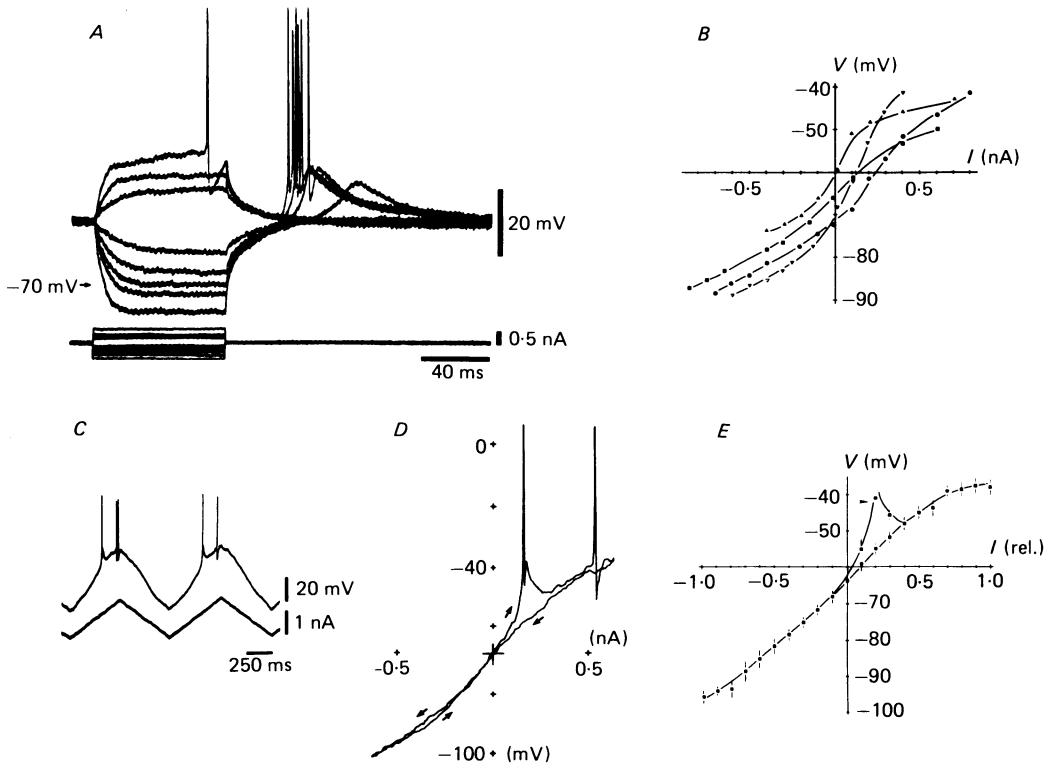

Fig. 1. Current–voltage relationship of thalamic neurones. *A*, response to injections of depolarizing and hyperpolarizing current pulses. The cell was depolarized from rest with a direct current injection in order to inactivate the low-threshold burst response. (The resting potential is indicated by a small arrow to the left in this and the following Figures.) Note the early break in the voltage trajectory followed by a slowly rising potential after the largest depolarizing pulse and the rebound burst responses after the hyperpolarizing pulses. *B*, current–voltage plots based on four different experiments similar to the one shown in *A*. The current–voltage curves all have a sigmoidal shape demonstrating double rectification. *C*, injection of 1 Hz double-ramp current. *D*, Lissajous figure based on the experiment shown in *C*. This experiment also demonstrates rectification across the membrane as well as hysteresis (the response to positive-going current is different from the response to the negative-going current). *E*, average of Lissajous figures from six cells. The small bars indicate the standard error of the mean for each point and the arrow head the threshold for the fast action potential. Each individual Lissajous figure was transformed before averaging to give the cell an input resistance of 40 MΩ at rest and the current was then set to an arbitrary value of ±1 peak to peak.

tested in a similar manner, the current–voltage relationship could be characterized as consisting of three components. Near the resting membrane potential (i.e. −65 mV) a depolarizing or a hyperpolarizing current pulse smaller than 0·1 nA produced a close to linear voltage displacement. As the amplitude of outward or inward current injections was made larger, the membrane conductance demonstrated both delayed and anomalous rectification.

Results obtained using a second test of the electrical properties of these cells are shown in Fig. 1*C–E*. Double-ramp currents with a trough to peak duration of

approximately 500 ms were injected intracellularly. As indicated in *C*, the current injection generated action potentials at two firing levels. In Fig. 1*D* the voltage generated by the double-ramp current was displayed in the x axis while the y axis of the cathode ray tube was driven by the current ramp itself. During the rising phase of the ramp current a sudden depolarization marked the l.t.s. described previously

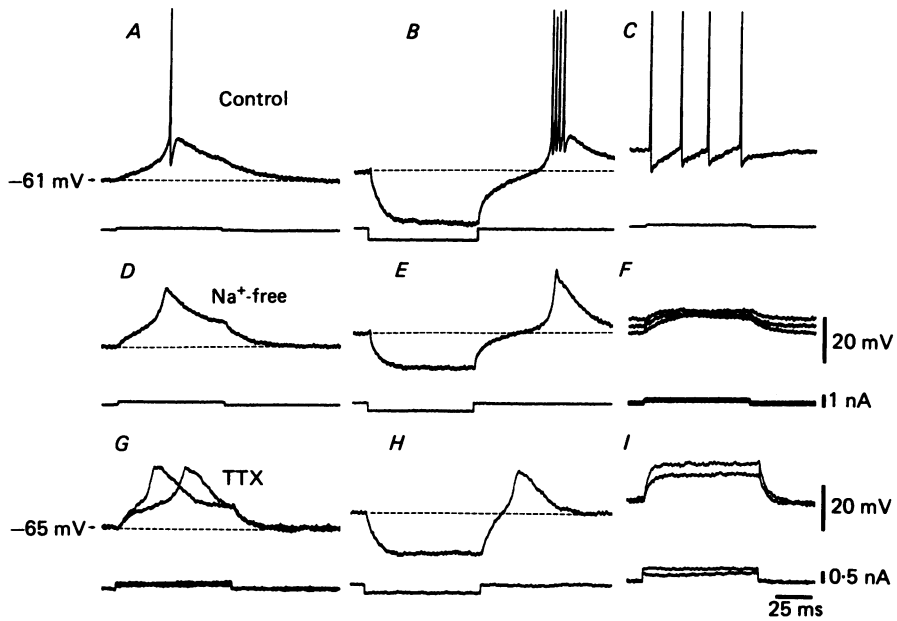

Fig. 2. Dependence of fast spikes on Na^+. *A*, *B* and *C*, control. Depolarizing current pulse from rest elicited a small burst response (*A*). Hyperpolarizing current pulse after d.c. depolarization of cell produced a rebound response (*B*), and a depolarizing pulse from a depolarized level elicited a train of fast spikes (*C*). *D*, *E* and *F*, after replacement of NaCl by choline Cl, the fast component of the burst response (*D* and *E*), and the fast action potentials (*F*) disappeared. The slow component of the burst was unchanged. *G*, *H* and *I*, in a different cell, tetrodotoxin (TTX) had the same effect as removal of NaCl.

(Jahnsen & Llinas, 1984) which often generated a fast action potential. This active upswing was always followed by a return of the membrane potential to a slowly rising depolarization indicating a sizeable rectification. With a large enough current a second action potential, having a different firing level, could be generated. The non-linearity which generates the low-threshold spike (l.t.s.) is absent in the falling component of the current injection.

Note that in Fig. 1*D* there is a crossing of the voltage trajectories at −68 mV. Thus, as shown above with square pulses, thalamic neurones demonstrate clear anomalous rectification and delayed rectification. Note in addition the marked hysteresis evident in Fig. 1*D*. Arrows in Fig. 1*D* indicate the direction of voltage change. The over-all membrane properties of these cells are further illustrated in Fig. 1*E* where the average current–voltage relationship for six cells was plotted in a manner similar to that used in Fig. 1*D*. These cells demonstrate two firing levels: the l.t.s. and the resulting burst response generated at the lower voltage level, and the tonic firing at the more depolarized membrane potential.

Ionic basis for generation of the fast action potential

By analogy with previous studies of mammalian neurones, the fast action potentials produced by direct depolarization or during the rebound response were assumed to be produced by an increased conductance to Na^+. Two types of experiments tested this hypothesis: (a) replacement of extracellular Na^+ with a non-conductive ion (Llinás & Sugimori, 1980*a*), and (b) bath application of tetrodotoxin (TTX) which is known to block g_{Na} in other C.N.S. neurones (Blankenship & Kuno, 1968; Blankenship, 1976; Ritchie & Rogart, 1977). An action potential generated by direct activation of a thalamic neurone from resting level is shown in Fig. 2*A*. The depolarization generates a l.t.s. and a fast action potential. As shown in Fig. 2*B*, following a hyperpolarizing pulse the membrane potential returned to base line with a concave trajectory followed by a rebound l.t.s. If the cell was depolarized from a more positive holding potential, tonic firing was elicited (Fig. 2*C*). Following replacement of Na^+ by choline, a current injection similar to that in Fig. 2*A* produced only the l.t.s. (*D*) without generating fast spikes. Similarly, if the cell was hyperpolarized with a current pulse (Fig. 2*E*), only a rebound l.t.s. was observed. A depolarizing current pulse superimposed on d.c. depolarization of the cell (Fig. 2*F*) also failed to produce repetitive firing as shown in Fig. 2*C*. The last row of Fig. 2(*G–I*) illustrates the results of a similar set of experiments in another neurone, following TTX administration. As in records *D–F* of Fig. 2 the results of such experiments indicate that the fast action potentals observed in thalamic neurones are produced by a TTX-sensitive voltage-dependent Na^+ conductance.

Voltage-dependent plateau potential

The second type of response observed upon depolarization of thalamic neurones is a slow plateau depolarization. This response can be large enough to be regenerative and has a threshold lower than that for the activation of the fast action potential (Jahnsen & Llinás, 1984). This plateau was best observed when the neurones were depolarized with a trapezoidal current injection (Fig. 3). If, using such a trapezoidal current and a cycle time of about 25 s, the membrane potential was brought from -80 to -40 mV, held at -40 mV, and then decreased to -80 mV, the thalamic neurones responded as shown in Fig. 3*A*. As the membrane was depolarized, the slope of the voltage trace demonstrated a sudden increase followed by repetitive firing. Similarly, as the current injection decreased, there was an initial rapid decay followed by a slower rate of change of the potential as it approached -80 mV. Addition of TTX to the bath (Fig. 3*B*) eliminated both the increase in slope seen during the rising and falling phases of current injection, and the fast action potentials. If the passive membrane response seen in Fig. 3*B* is subtracted from the active response in Fig. 3*A* (after filtering to eliminate the spikes), the component which generated the firing can be isolated (Fig. 3*C*) (the depression in the plateau being due to filtered spike after-hyperpolarization, a.h.p.). Note that this TTX-sensitive potential demonstrated a slow and graded onset and decay during the rising and falling phases of the current injection, indicating that at this level of depolarization the plateau potential was not regenerative. This graded depolarization is best seen in Fig. 3*D–F* where the extracellular Ca^{2+} was replaced by Co^{2+} and Mg^{2+}. Under these circumstances current

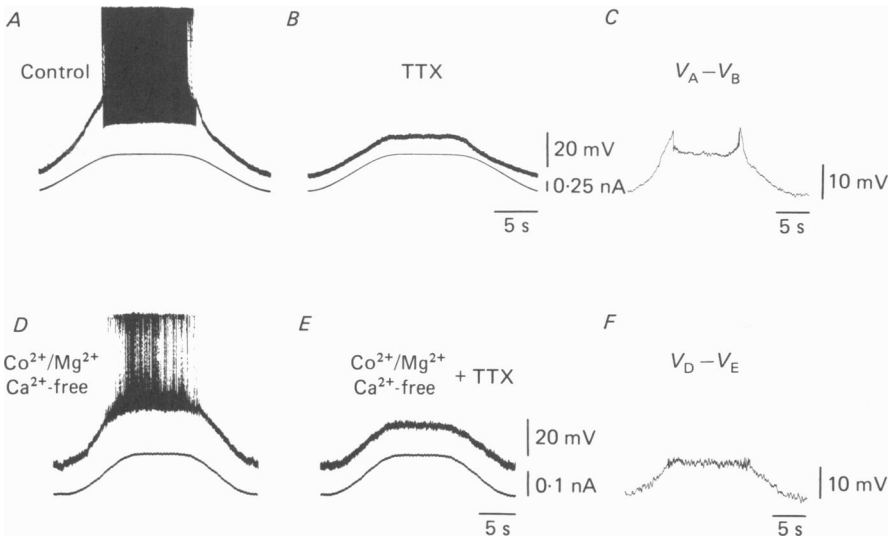

Fig. 3. Ionic basis for plateau potentials. *A*, injection of trapezoidal current pulse produced depolarization of the cell and a train of fast spikes, each followed by an after-hyperpolarization (a.h.p.). *B*, after addition of TTX, the fast spikes were blocked and the d.c. depolarization decreased. *C*, difference between the voltage responses before (A) and after (B) after low-pass filtering of the signals at 6 Hz. The difference is a TTX-sensitive plateau potential which is most likely produced by activation of a 'non-inactivating' Na^+ conductance. *D*, *E* and *F*, same experiment as in *A–C* but after Ca^{2+} conductance was blocked by Co^{2+}.

injections produced a response similar to that in *A*; however, the plateau action potentials were not followed by the large a.h.p.s seen in Fig. 3*A*. When TTX was added to the bath (Fig. 3*E*), both the action potentials and the plateau response were blocked. The plateau is shown in isolation in Fig. 3*F*. Similar results were obtained when Na^+ in the extracellular medium was replaced by choline. It may be concluded, therefore, that thalamic neurones dislay a voltage-dependant Na^+ conductance which does not inactivate rapidly. This conductance is blocked by TTX and has a lower threshold than that generating the fast action potentials.

Ionic conductances generating the low-threshold spike response

The similarities between l.t.s. described previously by Jahnsen & Llinás (1984) and the low-threshold Ca^{2+}-dependent spike in inferior olivary cells (Llinás & Yarom, 1981*a*, *b*) prompted us to investigate whether this response was Ca^{2+} dependent. A set of control potentials similar to those in Fig. 2 are shown in the upper part of Fig. 4. In Fig. 4*A*, depolarization of the cell from a resting level of −65 mV generated a typical burst response. A similar response was generated as a rebound from a hyperpolarizing current injection (Fig. 4*B*). In addition, at the break of the hyperpolarizing response the membrane potential returned to the base line with a concave trajectory. In Fig. 4*C*, repetitive firing was observed when the cell was depolarized from a resting level slightly more positive than that in Fig. 4*A* and *B*. Addition of Co^{2+} (2·3 mM) to the bath (known to block g_{Ca} in invertebrates (cf.

Hagiwara, 1973) and in mammalian neurones (Llinás & Sugimori, 1980*a*; Llinás & Yarom, 1981*b*)) and a reduction of the external Ca^{2+} concentration to 0·1 mM produced changes in the response to both depolarizing (Fig. 4*D*) and hyperpolarizing (Fig. 4*E*) current pulses. In the former case, the response had a higher threshold and consisted of a rather slow depolarization (the Na^+-dependent plateau response) upon which an action potential was generated (Fig. 4*D*). The return of the membrane

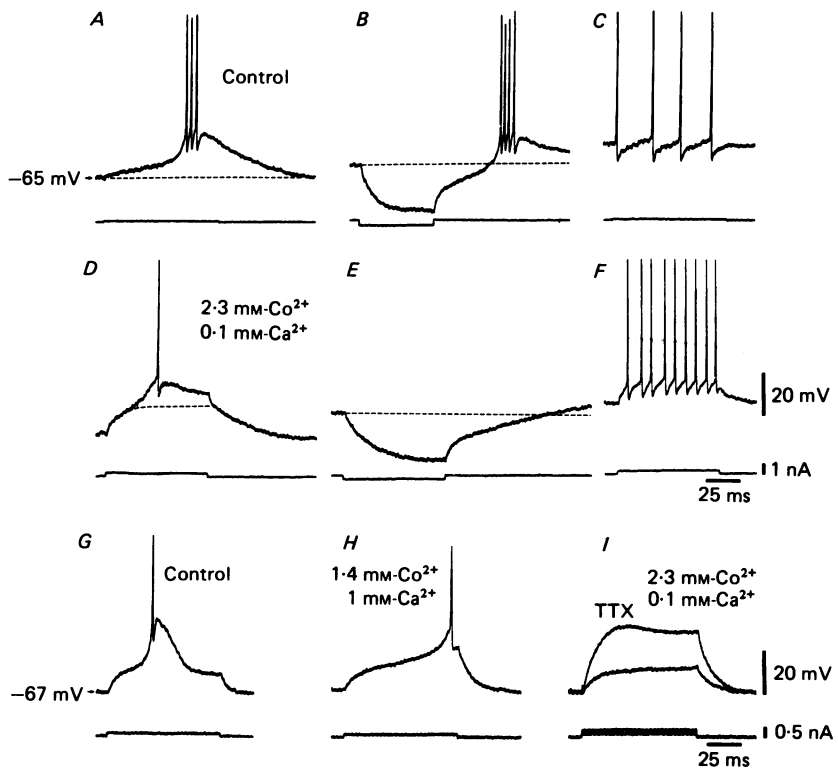

Fig. 4. Effect of blocking g_{Ca} on l.t.s. *A*, *B* and *C*, control responses. Burst response (*A*), rebound burst response (*B*), and fast spikes (*C*). *D*, *E* and *F*, 5 min after addition of Co^{2+} and reduction of Ca^{2+}, the burst response (at rest) (*D*) and the rebound response (*E*) are blocked but fast spikes are not affected (*D* and *F*). *G*, *H* and *I*, complete block of burst response in another cell after reduction of the Ca^{2+} concentration and addition of Co^{2+} to the solution. *G*, control response. *H*, after 15 min only the fast spike and a slowly rising potential remained. *I*, addition of TTX completely blocked the active responses.

potential following a hyperpolarizing pulse was slow (Fig. 4*E*) and no rebound potential was observed as compared with Fig. 4*B*. If the membrane was held depolarized and a square current pulse applied, the cell fired repetitively (Fig. 4*F*). (Note that for a similar level of depolarization the interspike intervals are decreased and the a.h.p. is smaller than in Fig. 4*C*.)

Blockage of the l.t.s. is shown in the last three records of Fig. 4. In this experiment, a square pulse applied to a cell held at a slightly hyperpolarized level generated a l.t.s. response (Fig. 4*G*). Following reduction of the Ca^{2+} concentration to 1·0 mM and the addition of Co^{2+} (1·4 mM) and to the bath, the l.t.s. was blocked but a slow

depolarizing potential and the fast spike remained (Fig. 4*H*). Application of TTX completely blocked these two responses (Fig. 4*I*). A similar block of the l.t.s. as seen in Fig. 4*H* was obtained in experiments where Mn^{2+} or Mg^{2+} was substituted for Ca^{2+} in the bathing solution and the preparation kept in this medium for 45 min.

These findings strongly indicate that the l.t.s. in thalamic cells is generated by a voltage-dependent Ca^{2+} conductance, very much as initially demonstrated in the

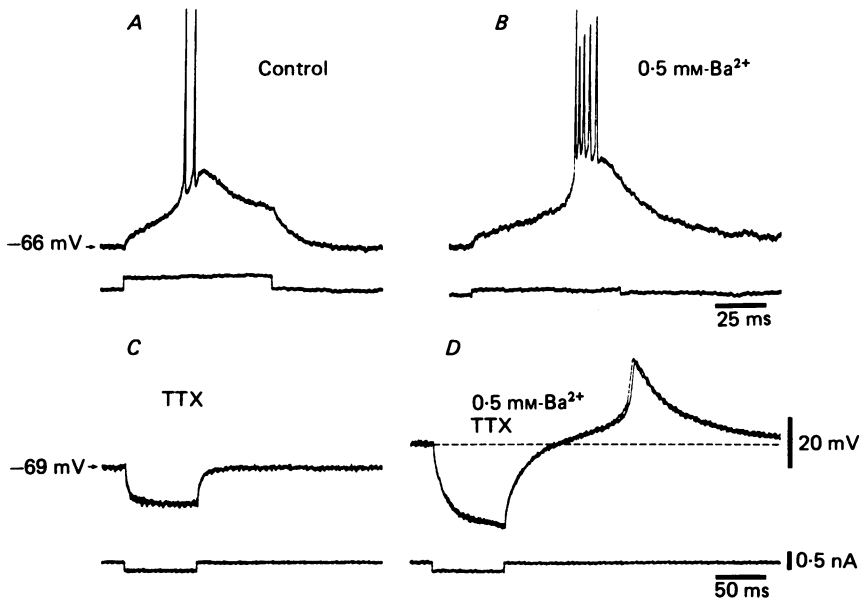

Fig. 5. Effect of Ba^{2+} on the burst response. *A*, control. *B*, replacement of 0·5 mM-Ca^{2+} with Ba^{2+} reduced the threshold for the burst response and depolarized the cell slightly. (This was compensated for in *B* by injecting a small hyperpolarizing holding current.) The amplitude of the l.t.s. and the number of action potentials increased leaving the burst duration unchanged. *C* and *D*, in the presence of TTX, Ba^{2+} increased the input resistance and depolarized the cell sufficiently to elicit a rebound l.t.s.

inferior olive (Llinás & Yarom, 1981*b*). This Ca^{2+} conductance inactivates when the membrane potential is positive to −55 mV and de-inactivates with hyperpolarization as shown in Fig. 5*B* in the accompanying paper (Jahnsen & Llinás, 1984). In addition, these experiments demonstrate that when the cell is depolarized in the absence of external Ca^{2+}, or following blockage of the slow Ca^{2+} conductance, the cells are still capable of generating a slow depolarization. This TTX-sensitive depolarization is the same as that described above as generating the plateau response (Fig. 3).

Barium ions. The ionic basis for the burst response was further studied by replacing some of the Ca^{2+} in the bath with Ba^{2+}. As shown in Fig. 5*A*, depolarization of the neurone generated a typical burst response. Addition of $BaCl_2$ to the bath produced a slight depolarization, a marked reduction in the l.t.s. threshold, and an increase in both its rate of rise and duration (Fig. 5*B*). The l.t.s. generated five action potentials rather than the two in Fig. 5*A*. Hyperpolarizing pulses were used to test the effects of TTX and Ba^{2+} (Fig. 5*C* and *D*). The control response is illustrated in Fig. 5*C*. As in Fig. 5*B*, Ba^{2+} produced a slight depolarization of the cell. Note that

the current injections used in Fig. 5*C* produced, in the presence of Ba^{2+} (Fig. 5*D*), a hyperpolarizing potential with an increased amplitude and a longer charging time. In addition, at the end of the pulse there was a clear rebound spike. This finding indicates that Ba^{2+} which can move through the Ca^{2+} channels (Werman & Grundfest, 1961; Hagiwara 1973), also moves through the channels responsible for the generation of the l.t.s., and that the falling phase of the l.t.s. is due to voltage-dependent inactivation and not to the presence of the Ca^{2+}-sensitive K^+ conductance $g_{K[Ca]}$ since this conductance is not activated by Ba^{2+} (Eckert & Lux, 1976). Moreover, the rather large increase in resistance suggests that as in other neurones (Eaton & Brodwick, 1980; Armstrong, Swenson & Taylor, 1982), Ba^{2+} has a direct blocking action on g_K.

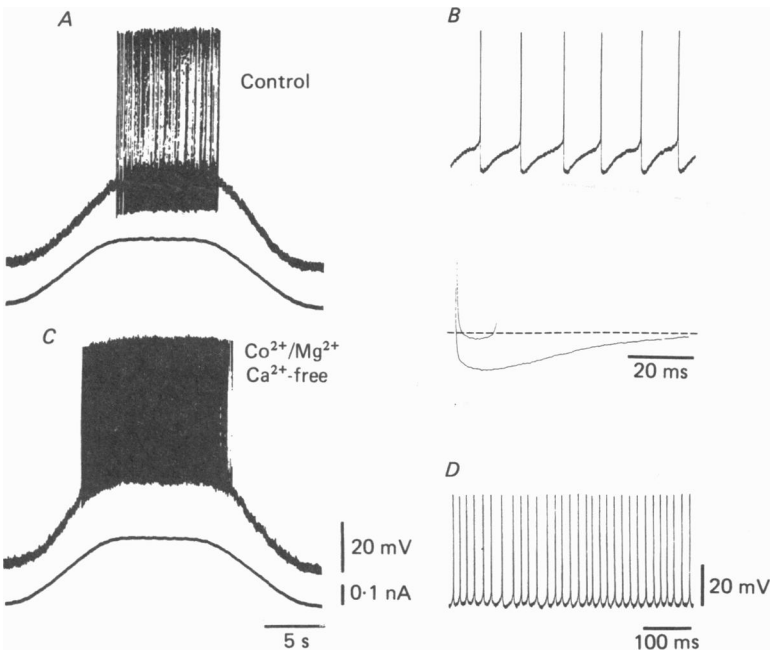

Fig. 6. Effect of blocking Ca^{2+} conductance on the after-hyperpolarization (a.h.p.). *A* and *B*, control, injection of a 25 s trapezoidal current produced repetitive firing followed by marked a.h.p. (*A*) (shown at a faster time base in *B*). *C* and *D*, after equimolar substitution of Ca^{2+} with Co^{2+} and Mg^{2+} the a.h.p.s are reduced and the firing frequency increased (*C*) (shown at a faster time base in *D*). A computer-calculated average of ten interspike intervals taken before and after the Ca^{2+} conductance was blocked are superimposed in the lower part of *B*.

Ionic basis for a.h.p.

The hyperpolarization which follows spike activation in thalamic neurones is an important component of the integrative properties of these cells. We expected this a.h.p. to be generated by a voltage-dependent K^+ conductance and by a Ca^{2+}-dependent K^+ conductance similar to those seen in hippocampal (Hotson & Prince, 1980), Purkinje (Llinás & Sugimori, 1980*a*) and inferior olivary neurones (Llinás & Yarom, 1981*b*). In order to ascertain whether this mechanism was present

in thalamic neurones, repetitive firing was evoked by trapezoidal current injection. At peak activation, as seen in Fig. 6*A*, each a.h.p. brought the membrane potential to approximately 15 mV below the firing level, the a.h.p. lasting approximately 100 ms. The details of the a.h.p., shown in Fig. 6*B*, reveal two components of the return voltage: an initial fast phase and a late slow phase. Following replacement of Ca^{2+} by Co^{2+} and Mg^{2+}, the neuronal response to the same current injection was

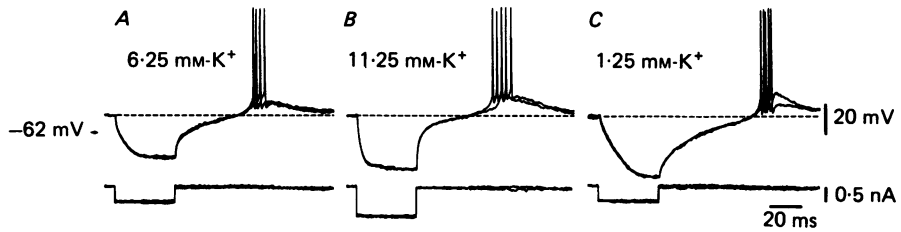

Fig. 7. Effect of changing external K^+ concentration on the response to hyperpolarizing pulses. *A*, control. *B*, increase in external K^+ concentration of 5 mM to 11·25 mM produces a reduction in the return of the potential to base line. *C*, reducing external K^+ concentration by 5 mM to 1·25 mM enhanced the delayed return to base line and reduced the l.t.s.

clearly modified (Fig. 6*C*). Thus, the firing level decreased and, for the same level of depolarization, a much faster firing frequency was observed. In addition, the a.h.p. (seen in Fig. 6*D*) was dramatically reduced and only a small, short-lasting (10 ms) a.h.p. remained. The difference between these two a.h.p.s is demonstrated in the lower part of Fig. 6*B* where the trajectories of the a.h.p. under both conditions are superimposed. Since with addition of Co^{2+} and Mg^{2+}, the large a.h.p. is not activated, an important component of this hyperpolarization must indeed be generated by a $g_{K[Ca]}$.

Another component observed following hyperpolarizing pulses (Figs. 2*B* and 4*B*) was the slow concave voltage return to base line (Llinas & Jahnsen, 1982). That this slow return is not due to $g_{K[Ca]}$ can be seen in Fig. 4*B* and *E* where blockage of Ca^{2+} conductance (Fig. 4*E*) removed the rebound response, without affecting the membrane potential trajectory. This indicates then that the slow return to base line is probably due to an early voltage-dependent K^+ conductance which becomes inactive.

The nature of this slow return to resting level was further studied by modifying the driving force for K^+ by producing either an increase (from 6·25 to 11·25 mM) or a decrease (to 1·25 mM) in the external K^+ concentration. These modifications produced a change of the a.h.p. without affecting either the firing of fast action potentials or the l.t.s. threshold (Fig. 7*A*). During both these experiments the membrane potential was actively held at the same level as before K^+ manipulation. In high K^+, a hyperpolarizing pulse (Fig. 7*B*) produced an increase in the rate of return of the potential to base line commensurate with the change in the K^+ equilibrium potential E_K. By contrast, a reduction of extracellular K^+ enhanced the slow return to base line (Fig. 7*C*) again commensurate with the change in driving force for K^+. It must be noted that although the somatic membrane voltage was held at the control level by a constant d.c. injection, the distant dendritic membrane of the neurones in Fig. 7*B* and *C* was probably more positive and more negative,

respectively, than in the control experiment. However, in both cases the direction of the inevitable error lends further support to our conclusion since such anisopotentiality would tend to diminish the effect of changing E_K, an effect which is nevertheless clearly demonstrated in Fig. 7*B* and *C*. In short then, the slow return of the membrane potential to base line following hyperpolarization is most clearly ascribed to the presence of a K^+ conductance similar to that described as the A current by Hagiwara, Kusano & Saito (1961), Connor & Stevens (1971) and Neher (1971). This conductance has been previously reported in vagal motoneurones (Yarom, Sugimori & Llinás, 1980) and more recently in hippocampal cells (Gustafsson, Galvan, Grafe & Wigström, 1982).

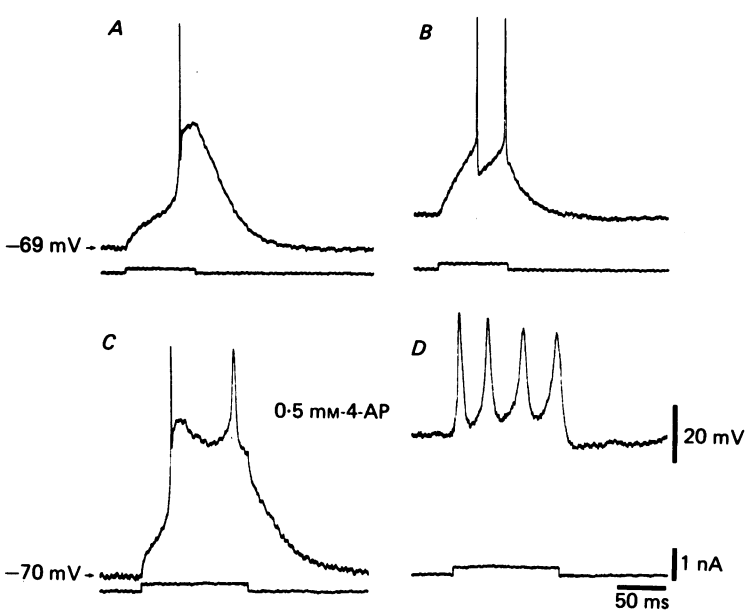

Fig. 8. High-threshold spikes. *A* and *B*, control. Stimulation with depolarizing current at rest (*A*) and at depolarized level (*B*). *C* and *D*, same experiment in a different cell after addition of 4-aminopyridine (4-AP). In *C*, a large, prolonged l.t.s. was elicited with a broad, slow-rising second spike. When the cell is depolarized to −20 mV in *D*, the same depolarizing pulse elicited four slow, broad action potentials.

High-threshold Ca^{2+} electroresponsiveness; dendritic spikes

Among the 229 recordings obtained from thalamic cells, a subset (twelve) demonstrated high-threshold Ca^{2+} spikes. Indeed, as seen in Fig. 8*A*, a depolarizing current pulse produced a clear l.t.s. from a rest potential of −69 mV. However, as the cell was depolarized from rest, two high-threshold, fast, all-or-none potentials followed by a hyperpolarization were observed (Fig. 8*B*). In another cell (Fig. 8*C*) addition of 4-aminopyridine (0·5 mM) produced a large increase of the response elicited from rest (−70 mV). In this case the amplitude and duration of the l.t.s. was increased and, in addition, a broad slow-rising action potential was observed on the shoulder of the prolonged l.t.s. The membrane potential returned to base line at the break of the current pulse. When the cell was depolarized to −20 mV the depolarizing current

pulse produced, rather than the response seen in Fig. 8*B*, four slow action potentials with an over-all duration of 18–22 ms and a peak-to-peak spike interval close to 30 ms (Fig. 8*D*). Results of experiments designed to determine the ionic basis for these high-threshold spikes are illustrated in Fig. 9. In Fig. 9*A* the extracellular Na^+ was replaced by choline. From a hyperpolarized level (−70 mV) a depolarizing pulse elicited a typical l.t.s. However, from a depolarized resting level the same current

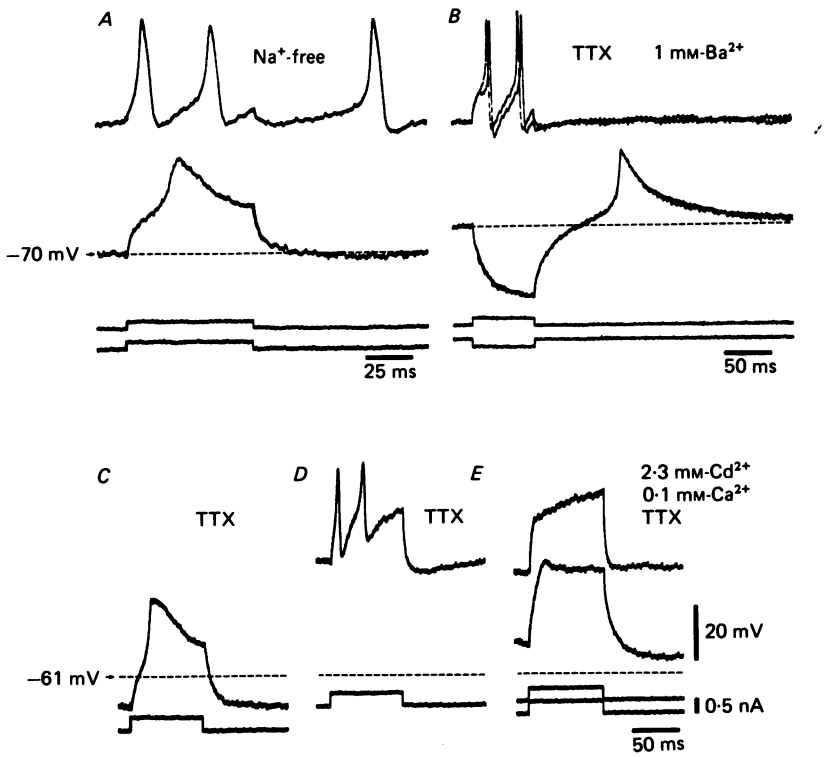

Fig. 9. Effect of replacing Na^+ or blocking g_{Na} on high-threshold spikes. *A*, after replacing NaCl with choline Cl, both the l.t.s. (second trace) and the high-threshold spike (h.t.s.) (top trace) could be elicited with the same current pulse depending on holding level. *B*, insensitivity of low-and high-threshold spikes to TTX and to Ba^{2+} (note time scale). *C*, *D* and *E*, sensitivity of the high-threshold spikes addition of Cd^{2+} to the bath. In *C* and *D*, controls in the presence of TTX. In *D*, substitution of 2·3 mM-ca^{2+} with Cd^{2+} completely abolished both h.t.s. and l.t.s.

elicited slow, small-amplitude action potentials similar to those seen in the presence of 4-aminopyridine. Similar responses were observed in the presence of TTX (Fig. 9*B*; note time scale). In this example, although 1 mM-Ca^{2+} was replaced with 1 mM-Ba^{2+}, the duration of the high-threshold spike did not increase, suggesting that in contrast to the high-threshold dendritic spike in inferior olivary neurones (Llinás & Yarom, 1981*a*, *b*), these potentials in thalamic neurones do inactivate. The Ca^{2+} dependence of both the low- and high-threshold spikes is illustrated in Fig. 9*C–E*. Addition of 2·3 mM-Cd^{2+} and reduction of Ca^{2+} abolishes both the low-threshold and the new high-threshold Ca^{2+} spikes (Fig. 9*E*).

TABLE 1. Values for resting potential, spike height, rate of rise and input for seven neural elements thought to be dendrites of thalamic neurones

Location	V_{rest} (mV)	V_{spike} (mV)	Rate of rise (V/s)	Input resistance (MΩ)
Posterolateral	61	89	198	127
group	67	79	159	148
Medial group	55	74	203	143
	57	65	116	88
	68	90	196	46
	58	80	174	67
	50	63	80	104
$n = 7$	59·4 ± 6·5†	77·1 ± 10·6*	160·9 ± 46·8‡	103·3 ± 38·7‡

* Not significantly different from cells in Table 1 of Jahnsen & Llinás (1984) (Wilcoxon).
† Significantly different at 5% level (Wilcoxon).
‡ Significantly different at 1% level (Wilcoxon).
All values are mean ± S.D.

The dendritic origin of these Ca^{2+}-dependent high-threshold spikes is supported by six lines of evidence: (1) their absence from the usual 'somatic' recordings (although observed at the somatic level after 4-aminopyridine), (2) the higher input resistance always observed under these circumstances (see Table 1), (3) the rather large depolarization required for their generation, clearly distinguishing them from the conductance which generates the l.t.s., (4) the similarity of the electrophysiological properties observed in these penetrations to presumed somatic recordings, including antidromic invasion, indicating that at least some are projection neurones rather than small interneurones, (5) the presence of Ca^{2+}-dependent K^+ conductance (which generates the a.h.p.) even under conditions where the low-threshold (i.e. somatic) rebound Ca^{2+} response would be inactivated, (6) their similarity to responses obtained from intradendritic recordings from Purkinje cells under direct vision (Llinás & Sugimori, 1980*b*).

Oscillatory behaviour

If certain electrophysiological conditions are met, the above properties of thalamic neurones coalesce to generate their oscillatory firing, as seen in Fig. 10. In this example the cell was depolarized slightly by a direct current which activated the slow Na^+ conductance. The direct current was then maintained and 0·5 ms pulses were delivered through the micro-electrode. As seen at a faster sweep speed (Fig. 10*a* and *b*), the membrane potential reached a point where a single stimulus produced a train of action potentials characterized by an initial spike, followed by a hyperpolarization itself followed by a rebound slow depolarization which, by activating an action potential, restarted the cycle. This self-regenerating process was repeated five times in succession in Fig. 10*b* following a single stimulus. This particular type of oscillatory behaviour may last for seconds and represents a stable functional state of these neurones in which the different ionic conductances are sequentially activated to produce an oscillatory firing at 9–11 Hz. Note that, as reported in the accompanying paper (Jahnsen & Llinas, 1984), if these cells are further depolarized, the firing frequency is directly related to the level of membrane depolarization. Thus, this 10 Hz

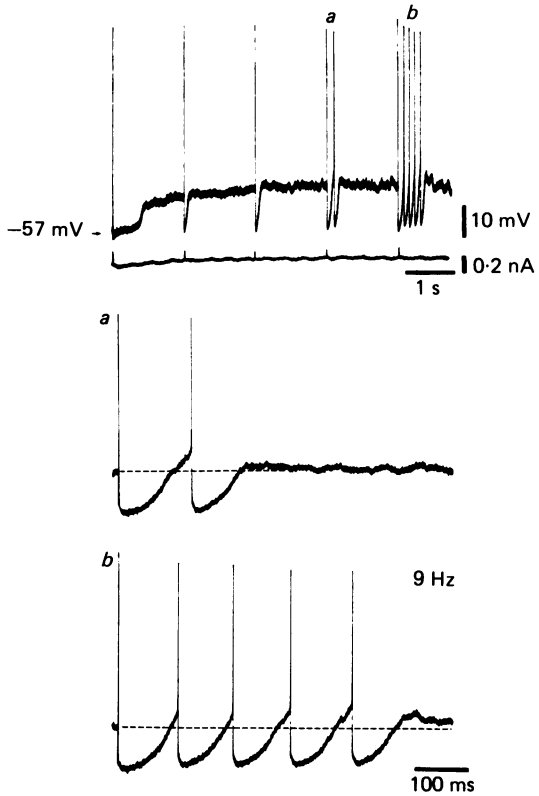

Fig. 10. 9 Hz oscillations in a thalamic neurone. The cell was depolarized from rest to −46 mV with injection of a direct current and stimulated with 0·5 ms intracellular current pulses which triggered self-maintained oscillation at 9 Hz after a single stimulus. The oscillations are shown at a faster time base in the lower part of the Figure.

rhythm may be converted into a higher level repetitive firing but only by further active depolarization of the neurone.

The two oscillatory rhythms of thalamic cells. Another approach to studying the oscillatory character of thalamic neurones is to activate a cell at different frequencies using double-ramp currents in order to determine whether there are optimum repetition rates for activating a particular set of electroresponsive properties. As shown in Fig. 11, double-ramp currents with a peak-to-peak frequency of 1,3,5,7 and 10 Hz were applied to a neurone. At 1 Hz the two different firing levels seen in Fig. 1 are illustrated. They characterized the burst response produced by the l.t.s. and the tonic discharge observed at more depolarized levels. At 3 Hz with a rate of rise of 0·6 V/s, these two firing levels are still clearly definable. The two thresholds converge until at 10 Hz, the repetition rate makes the l.t.s. difficult to elicit as would be expected from the duration of the refractory period for the l.t.s. (Jahnsen & Llinás, 1984). Lissajous figures for each frequency in another cell are shown at the right of each spike record. They demonstrate the change in depolarizing trajectory of the action potentials at different frequencies as well as the change in the return potential with increased rate of rise and fall. These experiments indicate that the response of

thalamic cells to a current ramp depends on the slope of the depolarization. Furthermore, the time and voltage dependence of l.t.s. de-inactivation and its prolonged recovery period, in conjunction with the I_A current, would generate an oscillatory frequency with an optimum interspike interval near 170 ms, giving an oscillatory frequency close to 6 Hz. On the other hand, from a more depolarized level, the rather stable oscillatory frequency of 9–11 Hz is elicited, as described above.

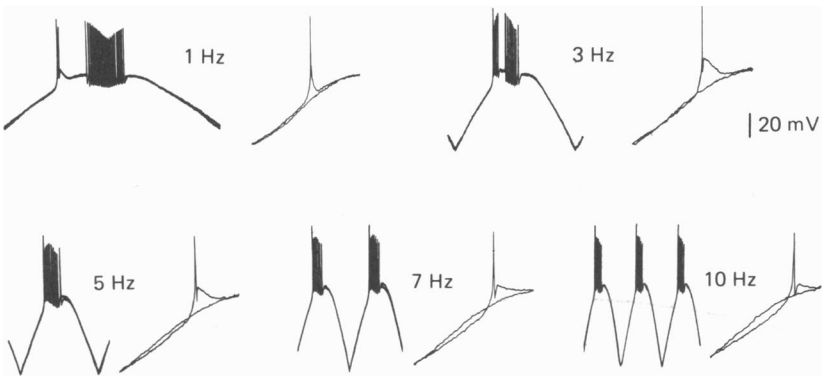

Fig. 11. Responses to injection of double-ramp currents at different frequencies. For each frequency, the membrane potential during double-ramp current injection is shown on the left, with a corresponding Lissajous figure taken from another cell to the right. Recordings on the left were obtained from a cell which fired both bursts and repetitive spikes during current injection. The Lissajous figures were constructed from recordings where the cell did not begin repetitive firing and where electrode rectification was minimal. Note that at frequencies slower than 7 Hz the burst response plays an important role in the initiation of firing but at higher frequencies the firing is dominated by the non-burst firing mode.

Combining the different electrophysiological properties of thalamic cells, one sees the two oscillatory properties described above. Thus, (a) the oscillatory behaviour seen in Fig. 10 was brought about at a membrane potential of −46 mV by a single action potential which triggered the oscillation as observed in Fig. 10*b*. (b) If the membrane is hyperpolarized and an action potential is generated by either a depolarizing potential or as a rebound response from the a.h.p. (see Fig. 12*b*), the recovery of the membrane is slowed by the I_A current and by $g_{K[Ca]}$ but the cell will fire very abruptly as the membrane potential reaches threshold for the l.t.s., which in turn can repeat the sequence. However, given the long inactivation for the l.t.s., the frequency of this oscillation, as described above, is slower (close to 6 Hz) than the 10 Hz seen at more depolarized levels. These two mechanisms of thalamic cell oscillation are illustrated in Fig. 12. In Fig. 12*A* the 10 Hz rhythm is produced by the rebound excitation due to the non-inactivating g_{Na}. In Fig. 12*B* the neurone oscillates at close to 6 Hz following rebound from a hyperpolarizing pulse after application of 0·5 mM-4-aminopyridine. This substance, which blocks g_K (Pelhate & Pichon, 1974; Llinás, Walton & Bohr, 1976; Yeh, Oxford, Wu & Narahashi, 1976; Meves & Pichon, 1977; Herman & Gorman, 1981), enhances the 6 Hz oscillatory behaviour by facilitating the h.t.s. and the $g_{K[Ca]}$ that follows. Increasing the $g_{K[Ca]}$ increases the duration and

magnitude of the a.h.p., making the rebound spike more likely by acting on both the voltage and the time dependence of Ca^{2+} conductance de-inactivation. Another experimental procedure to illustrate this oscillatory property is that of injecting periodic hyperpolarizing ramp currents which simulate inhibitory post-synaptic potentials (Fig. 12*C*). A clear oscillatory rhythm at 6 Hz is then observed. The diagram in Fig. 12*D* summarizes the mechanism involved in the generation of these two intrinsic rhythmic properties in thalamic neurones.

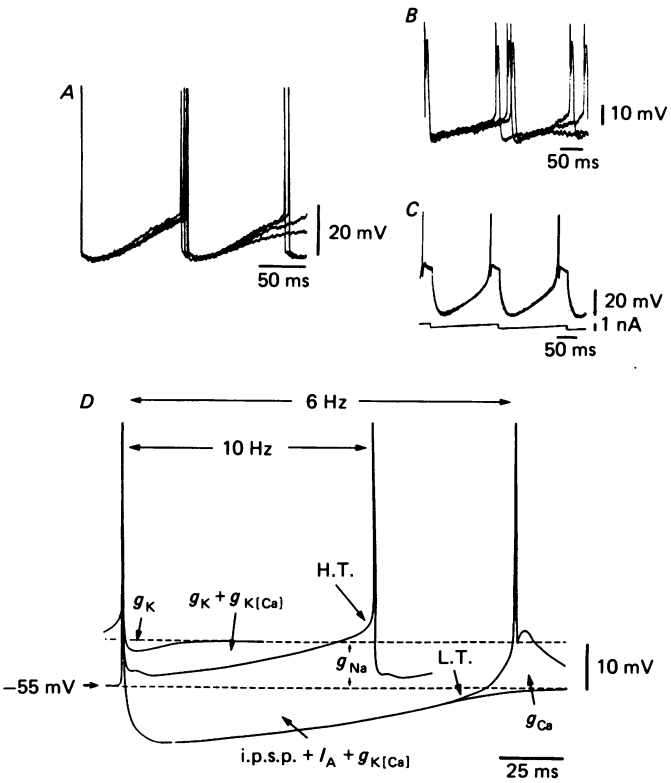

Fig. 12. Oscillatory properties of thalamic neurones. *A*, recording of 9–10 Hz oscillations similar to those demonstrated in Fig. 10. The fast Na^+ spike is followed by an after-hyperpolarization (a.h.p.) generated by a voltage-sensitive K^+ conductance (g_K), and a Ca^{2+}-dependent K^+ conductance ($g_{K[Ca]}$). The membrane potential is brought back to the threshold for the fast spike by the slow Na^+ conductance because the voltage-sensitive K^+ conductance is reduced after the preceding a.h.p. *B*, 6 Hz oscillation produced as a rebound response following a short hyperpolarizing pulse (not shown). This oscillation was facilitated by the presence of 4-AP in the bath. *C*, 6 Hz oscillation generated by ramp hyperpolarizing potentials. 6 Hz is the range frequency that the cells follow most readily. *D*, diagram of oscillatory mechanisms in the thalamus. In addition to the 10 Hz oscillations generated solely by the membrane conductance as shown in *A*, slower oscillations (about 6 Hz) can occur (shown in *B* and *C* by facilitating rebound excitation or by repeated hyperpolarizing potentials simulating i.p.s.p.s. The initial spike is followed by a marked hyperpolarization produced by a synaptic inhibition or by voltage- and Ca-dependent conductances. The hyperpolarization de-inactivates the transient K^+ current, I_A, which increases the duration of the a.h.p. This a.h.p. de-inactivates the low-threshold Ca^{2+} conductance generating a rebound l.t.s. which triggers the process once again (see text for further details). L.T. and H.T. are the threshold for l.t.s. and fast spikes respectively.

DISCUSSION

In the present investigation we have examined the ionic basis for the electro-responsive properties observed in thalamic neurones. In addition to the traditional Na^+ and K^+ conductances which generate the fast action potential (Hodgkin & Huxley, 1952), five conductances have been observed in these neurones. Together they generate the two types of firing typical of these cells.

Voltage-dependent conductances to Na^+

Thalamic neurones possess two different types of voltage-dependent Na^+ conductance. The first generates the fast action potential which characterizes the firing of axons and somata in most vertebrate and invertebrate neurones. The second type is characterized by a slow onset, a low threshold compared with that of the fast Na^+-dependent action potential, and by the lack of rapid inactivation. This conductance is similar to that originally observed in the Purkinje cell (Llinás & Sugimori, 1980*a*) and more recently in neocortical neurones (Stafstrom, Schwindt & Crill, 1982). It may also be akin to that recently reported for squid giant axons by Matteson & Armstrong (1982) where a slow Na^+ conductance is described as produced by 'sleepy' Na^+ channels, although their inactivation, even at low temperatures, is faster than that seen here. The 'non-inactivating' conductance of thalamic neurones becomes regenerative only under conditions where 'threshold' level is attained rapidly enough to develop a plateau equilibrium state with the g_K. If this state is not obtained, g_K will always obliterate regeneration although the threshold for non-inactivating g_{Na} is lower than that for g_K. The ultimate effect of these Na^+ conductances is then to serve as a graded boosting mechanism. The functional implication of such graded non-linearity deserves further analysis as it suggests rather complex integrative properties where the time-dependent component of this conductance far exceeds the passive time constant of the neurone. Indeed, while a slow depolarization would tend to bring the membrane potential closer to threshold and to fire the cell, at the same time the length constant is clearly reduced by the increased membrane conductance momentarily reducing the significance of remote synaptic input (see Fig. 1*B*, *D* and *E*).

Burst response

The burst response of thalamic neurones is similar to that seen in the inferior olive (Llinás & Yarom, 1981*a*, *b*). It is produced by Ca^{2+}-dependent l.t.s. responses which are blocked by the usual Ca^{2+} blockers, Co^{2+}, Cd^{2+} and Mn^{2+}, and abolished by the replacement of extracellular Ca^{2+} with Mg^{2+}. Furthermore, this potential can be generated when Ba^{2+} is substituted for Ca^{2+}. The voltage-dependent conductance which generates the l.t.s. is inactive at resting levels positive to -55 mV and is de-inactivated by membrane hyperpolarization. The time course for the action potential generated by this Ca^{2+} conductance is rather slow compared with that for the fast Na^+ spike. In general the bursts have a duration of 20–30 ms and are followed, as stated in the accompanying paper (Jahnsen & Llinas, 1984), by a refractory period.

After-hyperpolarization

The a.h.p. in thalamic cells is generated by three distinct mechanisms. A Ca^{2+}-dependent K^+ conductance increase which follows the activation of the fast spike and which is most probably related to Ca^{2+}-dependent spikes in the dendrites. In addition to this conductance, the a.h.p. – if large enough – is further enhanced by the I_A current. As in other neurones (Hagiwara *et al.* 1961; Connor & Stevens, 1971; Yarom, Sugimori & Llinás, 1980; Gustafsson *et al.* 1982), this conductance, inactive at depolarized membrane potential levels, is de-inactivated when the cell is hyperpolarized beyond rest level, resulting in a delayed return of the membrane to resting level, the time course being dictated by the closing kinetics of these K^+ channels. These two K^+ conductances are extremely important in regulating the firing frequency of thalamic neurones. Beyond these two conductances, when the cell is sufficiently depolarized to allow the slow Na^+ conductance to generate a plateau, the time dependence of the slow Na^+ conductance will also contribute to the time course of the upward trajectory of the a.h.p.

Dendritic spikes

As described above, thalamic neurones are capable of dendritic electroresponsiveness very much as observed in other mammalian neurones. The dendritic spikes do not seem to be as powerful as those in the inferior olive and, therefore, thalamic cells can fire at higher frequencies than inferior olive neurones. Primarily this is because the $g_{K[Ca]}$ is less prominent, although under normal conditions this component seems to be very important in the regulation of firing frequency (see Figs. 4*C* and 6*B*). In addition, as described in this paper, even in the presence of Ba^{2+} the 'dendritic' spike responses are not prolonged, suggesting a certain degree of inactivation of the dendritic Ca^{2+} spikes. This is in contrast to those observed in Purkinje (Llinás & Hess, 1976; Llinás & Sugimori, 1980*b*), inferior olivary cells (Llinás & Yarom, 1981*b*), hippocampal neurones (Schwartzkroin & Slawsky, 1978; Wong & Prince, 1978) and dorsal horn neurones (Murase & Randić, 1983). Thalamic dendritic spikes can be generated after TTX poisoning of the neurones under conditions where dendritic activation is likely to occur (i.e. possible intradendritic recording or bath addition of 4-aminopyridine).

Ionic basis for thalamic oscillation. Thalamic neurones appear to have two distinct and intrinsic ionic mechanisms capable of producing stereotyped oscillatory firing. These mechanisms are triggered at different membrane potential levels.

The first mechanism of oscillation in thalamic neurones occurs at a slightly depolarized level from rest and involves the activation of the slow Na^+ conductance. When cells are depolarized sufficiently and a suprathreshold stimulus is applied, action potentials followed by prolonged a.h.p.s are elicited. These a.h.p.s show a depolarizing overshoot produced in this case by the activation of the slow Na^+ conductance. If the slow Na^+ rebound is powerful enough, long trains of oscillatory responses may be obtained following a single stimulus. This oscillation has a mean cycle period of approximately 9–11 Hz. Because the hyperpolarization that follows these spikes is usually not deep enough to produce de-inactivation of the l.t.s. response mechanism, this oscillatory behaviour is modulated by the duration of the

a.h.p. and the slow Na^+ conductance. In this case the a.h.p. is produced, as stated above, by g_K and by the $g_{K[Ca]}$ which follows the l.t.s.

The second mechanism for intrinsic oscillation is observed if the membrane potential is sufficiently hyperpolarized, either by a direct current following a transient hyperpolarization or if g_K is modified such that dendritic spikes can be more easily activated from the soma. Under these conditions thalamic cells tend to produce 'off' responses upon release from this hyperpolarization. These 'off' responses, known as 'rebound potentials', have a refractory period such that they tend to drive thalamic neurones with a frequency of 5–6 Hz. This can be directly verified by the application of double-ramp pulses as shown in Fig. 11. The limit of this particular cycle is then given by the refractory period of the rebound Ca^{2+} spike and by the fact that its free-run interval tends to be close to 170 ms, at which time the rebound spike is fully de-inactivated, as determined by the double activation of the cells (Jahnsen & Llinás, 1984). This oscillatory rhythm is controlled by four mechanisms, the $g_{K[Ca]}$ produced by the l.t.s., the I_A, the time course of the recovery of the l.t.s., and the $g_{K[Ca]}$ produced by an increased dendritic Ca^{2+} spiking. Ultimately then the ionic conductances which trigger the firing of the thalamic neurones may be divided into two general groups: (a) those generated by the powerful excitatory rebound produced by the inactivating somatic Ca^{2+} conductance, and (b) those generated by the rebound of the less powerful mechanisms relating to the non-inactivating Na^+ conductance.

Oscillatory mechanisms in the thalamus

The present study demonstrates that thalamic neurones, regardless of location, are endowed with a set of ionic conductances that provide them with different forms of electroresponsiveness. We have referred to them in this paper as tonic firing and burst behaviour. These different functional states are regulated by membrane potential and *in vivo* most certainly by chemical modulators as indicated by the wake–sleep cycle. The central issue here, however, is that the distinct oscillatory behaviours of single cells are not generated as hypothesized in years past by the network properties such as recurrent excitation and inhibition (Andersen & Sears, 1964; Andersen, Brooks, Eccles & Sears 1964). Rather the cells themselves have a sufficient complement of voltage- and Ca^{2+}-dependent conductances to generate the 5–6 Hz oscillation characteristic of the θ rhythm (as in Parkinson's tremor) and the 10 Hz oscillatory firing characteristic of the α rhythm (Adrian & Matthews, 1934; Andersen & Sears, 1964). That these cells are capable of being tonically active (a functional state most probably subserving the so-called desynchronized brain activity) and also capable of demonstrating the two oscillatory rhythms described above implies that the determining parameters in these functional states are the biophysical properties intrinsic to these neurones. That such intrinsic properties would be finely tuned and modulated by the afferents or by recurrent systems cannot be denied. This is especially clear since the rhythmicity observed in the thalamus *in vivo* must be subserved by a superimposed system capable of incorporating these single cell oscillators into the synchronized ensemble firing which underlies the α and θ rhythms recorded from the scalp or the tremor observed in Parkinson's Disease.

Research was supported by United States Public Health Service program grant NS-13742 from the National Institute of Neurological and Communicative Disorders and Stroke. H. Jahnsen was

also supported by grants from the University of Copenhagen, the Danish Medical Research Council, the Weimann Fdn. and by an Albert Cass Traveling Fellowship.

REFERENCES

ADRIAN, E. D. & MATTHEWS, B. H. C. (1934). The Berger rhythm: Potential changes from the occipital lobes in man. *Brain* **57** (4) 355–385.

ANDERSEN, P., BROOKS, C. McC., ECCLES, J. C. & SEARS, T. A. (1964). The ventro-basal nucleus of the thalamus: potential fields, synaptic transmission and excitability of both presynaptic and post-synaptic components. *J. Physiol.* **174**, 348–369.

ANDERSEN, P. & SEARS, T. A. (1964). The role of inhibition in the phasing of spontaneous thalamo-cortical discharge. *J. Physiol.* **173**, 459–580.

ARMSTRONG, C. M., SWENSON, R. P., JR. & TAYLOR, S. R. (1982). Block of squid axon K channels by internally and externally applied barium ions. *J. gen. Physiol.* **80**, 663–682.

BLANKENSHIP, J. E. (1976). Tetrodotoxin: From poison to powerful tool. *Perspect. Biol. Med.*, **19**, 509–526.

BLANKENSHIP, J. E. & KUNO, M. (1968). Analysis of spontaneous subthreshold activity in spinal motoneurons of the cat. *J. Neurophysiol.* **31**, 196–209.

CONNOR, J. A. & STEVENS, C. F. (1971). Voltage clamp studies of a transient outward membrane current in gastropod neural somata. *J. Physiol.* **213**, 21–30.

EATON, D. C. & BRODWICK, M. S. (1980). Effects of barium on the potassium conductance of squid axon. *J. gen. Physiol.* **75**, 727–750.

ECKERT, R. & LUX, H. D. (1976). A voltage-sensitive persistent calcium conductance in neuronal somata of *Helix*. *J. Physiol.* **254**, 129–151.

GUSTAFSSON, B., GALVAN, M., GRAFE, P. & WIGSTRÖM, H. (1982). A transient outward current in a mammalian central neurone blocked by 4-aminopyridine. *Nature, Lond.* **299**, 252–254.

HAGIWARA, S. (1973). Ca spikes. *Adv. Biophys.* **4**, 71–102.

HAGIWARA, S., KUSANO, K. & SAITO, N. (1961). Membrane changes of *Onchidium* nerve cell in potassium-rich media. *J. Physiol.* **155**, 470–489.

HERMAN, A. & GORMAN, A. L. F. (1981). Effects of 4-aminopyridine on potassium currents in a molluscan neuron. *J. gen. Physiol.* **78**, 63–86.

HODGKIN, A. L. & HUXLEY, A. F. (1952). A quantitative description of membrane current and its application to conduction and excitation in nerve. *J. Physiol.* **117**, 500–544.

HOTSON, J. R. & PRINCE, D. A. (1980). A calcium-activated hyperpolarization follows repetitive firing in hippocampal neurons. *J. Neurophysiol.* **43**, 409–419.

JAHNSEN, H. & LLINÁS, R. (1982). Electrophysiological properties of guniea-pig thalamic neurons studied *in vitro*. *Neurosci. Abstr.* **8**, 413.

JAHNSEN, H. & LLINÁS, R. (1984). Electrophysiological properties of guinea-pig thalamic neurones: an *in vitro* study. *J. Physiol.* **349**, 205–226

LLINÁS, R. & HESS, R. (1976). Tetrodotoxin-resistant dendritic spikes in avian Purkinje cells. *Proc. natn. Acad. Sci. U.S.A.* **73**, 2520–2523.

LLINÁS, R. & JAHNSEN, H. (1982). Electrophysiology of mammalian thalamic neurones *in vitro*. *Nature, Lond.* **297**, 406–408.

LLINÁS, R. & SUGIMORI, M. (1980*a*). Electrophysiological properties of *in vitro* Purkinje cell somata in mammalian cerebellar slices. *J. Physiol.* **305**, 171–195.

LLINÁS, R. & SUGIMORI, M. (1980*b*). Electrophysiological properties of *in vitro* Purkinje cell dendrites in mammalian cerebellar slices. *J. Physiol.* **305**, 197–213.

LLINÁS, R., WALTON, K. & BOHR, V. (1976). Synaptic transmission in squid giant synapse after potassium conductance blockage with external 3- and 4-aminopyridine. *Biophys. J.* **16**, 83–86.

LLINÁS, R. & YAROM, Y. (1981*a*). Electrophysiology of mammalian inferior olivary neurones *in vitro*. Different types of voltage-dependent ionic conductances. *J. Physiol.* **315**, 549–567.

LLINÁS, R. & YAROM, Y. (1981*b*). Properties and distribution of ionic conductances generating electroresponsiveness of mammalian inferior olivary neurones *in vitro*. *J. Physiol.* **315**, 569–584.

MATTESON, D. R. & ARMSTRONG, C. M. (1982). Evidence for a population of sleepy sodium channels in squid axon at low temperature. *J. gen. Physiol.* **79**, 739–758.

MEVES, H. & PICHON, Y. (1977). The effect of internal and external 4-aminopyridine on the potassium currents in intracellularly perfused squid giant axons. *J. Physiol.* **268**, 511–532.

MURASE, K. & RANDIĆ, M. (1983). Electrophysiological properties of rat spinal dorsal horn neurones *in vitro*: calcium-dependent action potentials. *J. Physiol.* **334**, 141–153.

NEHER, E. (1971). Two fast transient current components during voltage clamp on snail neurons. *J. gen. Physiol.* **58**, 36–53.

PELHATE, M. & PICHON, Y. (1974). Selective inhibition of potassium current in the giant axon of the cockroach. *J. Physiol.* **242**, 90–91*P*.

RITCHIE, J. M. & ROGART, R. B. (1977). The binding of saxitoxin and tetrodotoxin to excitable tissue. *Res. Physiol. Biochem. Pharmacol.* **79**, 1–50.

SCHWARTZKROIN, P. A. & SLAWSKY, M. (1977). Probable calcium spikes in hippocampal neurons. *Brain Res.* **135**, 157–161.

STAFSTROM, C. E., SCHWINDT, P. C. & CRILL, W. E. (1982). Negative slope conductance due to a persistent subthreshold sodium current in cat neocortical neurons *in vitro*. *Brain Res.* **236**, 221–226.

WERMAN, R. & GRUNDFEST, H. (1961). Graded and all-or-none electrogenesis in arthropod muscle. II. The effects of alkali-earth and onium ions on lobster muscle fibres. *J. gen. Physiol.* **44**, 997–1027.

WONG, R. K. S. & PRINCE, D. A. (1978). Participation of calcium spikes during intrinsic burst firing in hippocampal slices. *Brain Res.* **159**, 385–390.

YAROM, Y., SUGIMORI, M. & LLINÁS, R. (1980). Inactivating fast potassium conductance in vagal motoneurons in guinea pigs: an in vitro study. *Neurosci. Abstr.* **6**, 198.

YEH, J. Z., OXFORD, G. S., WU, C. H. & NARAHASHI, T. (1976). Dynamics of aminopyridine block of potassium channels in squid axon membrane. *J. gen. Physiol.* **68**, 519–535.